

Quadrupole pairing interaction and signature inversion

F.R. Xu^{1,2}, W. Satulá,^{1,3} and R. Wyss^{1,4}

¹*Royal Institute of Technology, Physics Department Frescati,
Frescativägen 24, S-104 05 Stockholm, Sweden*

²*Department of Technical Physics, Peking University, Beijing 100871, China*

³*Institute of Theoretical Physics, University of Warsaw, ul. Hoża 69, PL-00 681 Warsaw, Poland*

⁴*Department of Technology, Kalmar University, Box 905, 391 29 Kalmar*

The signature inversion in the $\pi h_{11/2} \otimes \nu h_{11/2}$ rotational bands of the odd-odd Cs and La isotopes and the $\pi h_{11/2} \otimes \nu i_{13/2}$ bands of the odd-odd Tb, Ho and Tm nuclei is investigated using pairing and deformation self-consistent mean-field calculations. The model can rather satisfactorily account for the anomalous signature splitting provided that spin assignments in some of the bands are revised. Our calculations show that signature inversion can appear already at axially symmetric shapes. It is found that this is due to the contribution of the $(\lambda\mu) = (22)$ component of the quadrupole-pairing interaction to the mean-field potential.

PACS numbers: 21.60.Ev, 21.10.Re, 27.60.+j, 27.70.+q

Keywords: Quadrupole pairing interaction, Signature inversion, Rotational band, TRS-calculations.

I. INTRODUCTION

The invariance of the intrinsic Hamiltonian with respect to the signature symmetry gives rise to the occurrence of two rotational bands in odd and odd-odd nuclei that differ in spin by $1\hbar$. These bands are built upon the same intrinsic configuration but differ in their signature symmetry eigenvalue, r [1]. Often the signature exponent α [$I \equiv \alpha \pmod{2}$] is used to label these bands where α is related to r via $r = e^{-i\pi\alpha}$.

In general, signature partner bands are not equivalent energetically. The energy difference is called signature splitting when measured in the rotating frame of reference as a function of frequency. The origin of the splitting is essentially due to the mixing of the $\Omega = 1/2$ state into wave function. Since this component has a non-zero diagonal matrix element of the cranking operator $\omega \hat{j}_x$ of opposite sign for each signature, one expects one signature to gain (or lose) energy with increasing frequency with respect to the other. For high- j one-quasiparticle (1-qp) unique-parity configurations, the favored signature is obtained by the simple rule, $\alpha_f = (-)^{j-1/2} 1/2$ [2]. However, in unique parity 2-qp configuration in odd-odd nuclei, it may occur that $\alpha_f = (-)^{j\nu-1/2} 1/2 + (-)^{j\pi-1/2} 1/2$ band may become energetically unfavored. Similar effects have been observed in some odd-A nuclei in 3-qp configuration [3]. This phenomenon is called signature inversion [4].

Signature inversion has been observed, for example, in odd-odd nuclei for the $\pi h_{11/2} \otimes \nu h_{11/2}$ configurations in the $A \sim 130$ and $\pi h_{11/2} \otimes \nu i_{13/2}$ configurations in $A \sim 160$ regions. Different theoretical attempts have been presented to interpret the phenomenon. Triaxiality of the nuclear shape was suggested in Refs. [5,6,7,4]. The general condition for signature inversion to take place [4] was positive triaxial deformation, $\gamma > 0$, within the Lund convention combined with a specific position of the Fermi surface, see also [8,9]. One should point out, however, that (i) the γ -values are almost impossible to measure directly in experiment; (ii) the values of the γ parameter necessary to account for the experimental data are not always supported by potential energy calculations which in many cases predicts almost axial shapes [10]. Triaxiality seems, therefore, to be not always sufficient calling for alternative or supplementary mechanism.

Hamamoto [11] and Matsuzaki [12] analyzed the long-range, residual proton-neutron (pn) $\chi Q_p Q_n$ interaction. They concluded that the self-consistent value of the strength parameter χ is far too weak to account for the empirical data. Semmes and Ragnarsson [13] considered a residual pn contact force with spin-spin interaction, $V_{pn} \propto \delta(\mathbf{r}_p - \mathbf{r}_n)(u_0 + u_1 \vec{\sigma}_n \cdot \vec{\sigma}_p)$, in the framework of the particle-rotor model. Remarkably, using one set of parameters u_0, u_1 , it appeared possible to reproduce very accurately some $\pi h_{11/2} \otimes \nu h_{11/2}$ bands in the $A \sim 130$ region and $\pi h_{11/2} \otimes \nu i_{13/2}$ bands in rare-earth nuclei, without invoking triaxiality [10,14]. However, to account for the $\pi h_{9/2} \otimes \nu i_{13/2}$ bands in rare-earth nuclei, a substantial reduction of the strength parameters u_0 and u_1 was necessary [15]. Signature inversion is also obtained in the projected shell-model at axial symmetric shapes, resulting from the crossing of different bands with opposite signature dependence [16].

Another probe of the mechanism behind signature inversion are the electromagnetic transition amplitudes. The ratios of the BM1/BE2 transition rates are very sensitive to the deformation parameters (γ and β) and whether the decay goes from favored states to unfavored or vice versa [3]. In the present paper, however, we restrict ourselves

entirely to the systematics of Routhians and spins. Calculations of BM1/BE2 ratios are beyond the scope of this work.

In Ref. [17] we have published the results of deformation and pairing self-consistent Total Routhian Surface (TRS) calculations for ^{120}Cs . It has been demonstrated that the inclusion of quadrupole pairing correlations (QQ -pairing), number projection and a proper treatment of blocking into the TRS model made it possible to reproduce signature inversion without invoking the pn interaction. In this paper, we demonstrate that our extended TRS model is able to reproduce rather accurately and systematically the signature inversion in odd-odd $^{120-124}\text{Cs}$, $^{124-128}\text{La}$, $^{154-158}\text{Tb}$, $^{156-160}\text{Ho}$ and $^{158-162}\text{Tm}$ nuclei and that the mechanism causing signature inversion is triaxiality combined with the contribution of the $(\lambda\mu) = (22)$ component of the QQ -pairing force to the single-particle potential.

In the next section, we present a brief outline of our model. A general discussion on the role of the QQ -pairing force with respect to signature inversion is given in Sec. III. The discussion of empirical spin assignments and the results of self-consistent TRS calculations are presented in Sec. IV for the odd-odd $^{120-124}\text{Cs}$, $^{124-128}\text{La}$, $^{154-158}\text{Tb}$, $^{156-160}\text{Ho}$ and $^{158-162}\text{Tm}$ nuclei. A summary is given in the last section.

II. THE MODEL

The TRS method [18] is a macroscopic-microscopic approach in a uniformly-rotating body-fixed frame of reference [19]. The total Routhian of a nucleus is calculated on a grid in deformation space, using the Strutinsky shell correction method [20]. The model employs the deformed Woods-Saxon potential of Ref. [21] and liquid-drop model of Ref. [22]. The pairing energy is calculated using a separable interaction of seniority and doubly-stretched quadrupole type:

$$\bar{v}_{\alpha\beta\gamma\delta}^{(\lambda\mu)} = -G_{\lambda\mu} g_{\alpha\bar{\beta}}^{(\lambda\mu)} g_{\gamma\bar{\delta}}^{*(\lambda\mu)}, \quad (1)$$

where

$$g_{\alpha\bar{\beta}}^{(\lambda\mu)} = \begin{cases} \delta_{\alpha\bar{\beta}}, & \lambda = 0, \quad \mu = 0 \\ \langle \alpha | \hat{Q}_{\mu}'' | \bar{\beta} \rangle, & \lambda = 2, \quad \mu = 0, 1, 2. \end{cases} \quad (2)$$

The above expression employs good signature basis [23], $\bar{\alpha} = \hat{T}\alpha$ stands for the time-reversed state and $|\overline{r = \pm i}\rangle = \pm|r = \mp i\rangle$. To avoid the sudden collapse of pairing correlations, we use the Lipkin-Nogami approximate number projection [24]. It is important to stress that the model is *free* of adjustable strength parameters. The monopole pairing strength, G_{00} , is determined by the average gap method of Ref. [25] and the QQ -pairing strengths, $G_{2\mu}$, are calculated to restore the Galilean invariance broken by the seniority pairing force, see the prescription in Ref. [26]. For example, in the $A \sim 130$ mass region, where the 56(66) lowest proton (neutron) single-particle levels are used for the pairing calculation, the pairing strengths parameters are equal $G_{00} \approx 165(145)$ keV and $G_{2\mu} \approx 4.4(3.3)$ keV/fm⁴ for protons (neutrons). In the $A \sim 160$ mass region, single-particle levels between 10-70(15-90) were used for the pairing calculations for protons (neutrons) and typical values of the strength parameters are $G_{00} \approx 140(105)$ keV and $G_{2\mu} \approx 3.0(1.6)$ keV/fm⁴ for protons (neutrons). Let us recall that the use of the double-stretched generators for the QQ -pairing force result in, to a large extent, isotropic and shape independent values of $G_{2\mu}$ [27].

The resulting cranked-Lipkin-Nogami (CLN) equation takes the form of the well known Hartree-Fock-Bogolyubov-like (HFB) equation. In the TRS model, the CLN equation is solved self-consistently at each frequency and each grid point in deformation space which includes quadrupole β_2, γ and hexadecapole β_4 shapes (pairing self-consistency). Finally, the equilibrium deformations are calculated by minimizing the total Routhian with respect to the shape parameters (shape self-consistency). For further details concerning the formalism, we refer the reader to Ref. [28,29,30].

III. THE INFLUENCE OF THE QUADRUPOLE PAIRING FORCE ON SIGNATURE INVERSION

In our previous works [29,31], it has been shown that QQ -pairing, in particular its time-odd Δ_{21} component, plays an important role in the alignment of quasi-particles. It strongly influences the moment of inertia and partly can account for twinning of the spectra of odd and even super-deformed nuclei in the $A \sim 190$ mass region. The two-body pairing interaction enters also the single-particle channel via the Γ potential:

$$\Gamma_{\alpha\bar{\beta}}^{(\lambda\mu)} = -G_{\lambda\mu} \sum_{\gamma\delta>0} g_{\alpha\bar{\gamma}}^{(\lambda\mu)} g_{\bar{\beta}\delta}^{*(\lambda\mu)} \rho_{\delta\gamma}, \quad (3)$$

where ρ is the density matrix. The single-particle contribution coming from the separable pairing force is usually small and in many applications simply disregarded. However, in the Lipkin-Nogami approach, it has to be taken into account for the consistency of the method. Interestingly, in spite of its weakness, the $\Gamma^{(22)}$ field plays a rather important role for the signature inversion as will be demonstrated in the following.

Let us consider an odd-odd nucleus with an unpaired proton and neutron occupying the high- j , unique-parity orbits. The favored signature is expected to be $\alpha_f = (-)^{j_\pi - 1/2} 1/2 + (-)^{j_\nu - 1/2} 1/2$. However, when one of the particles is low in the shell and the other occupies orbits around the middle or above the middle of the shell, signature inversion can occur. In the $A \sim 130$ region e.g., two signatures, $\alpha_{f(u_f)} = (\alpha_\pi = -1/2) \otimes (\alpha_\nu = \mp 1/2) = 1(0)$, of the $\pi h_{11/2} \otimes \nu h_{11/2}$ configuration are seen in experiment. For the protons, only the signature-favored $\alpha_\pi = -1/2$ orbit is observed since the signature splitting of $\pi h_{11/2}$ low- Ω levels is typically several hundred keV. For instance, in ^{120}Cs , it is calculated to be more than 0.7 MeV at $\hbar\omega = 0.2$ MeV. The role of this low- Ω , high- j orbit is to induce a deformation close to axial symmetry with slight tendency towards positive γ value [4]. Otherwise it acts as spectator and the signature splitting is entirely due to the neutrons.

Fig. 1 shows the influence of each $Q_{2\mu}$ ($\mu = 0, 1, 2$) component of the QQ -pairing interaction on the signature splitting $\Delta e' \equiv e^{(u_f, \alpha=0)} - e^{(f, \alpha=1)}$, between the unfavored $e^{(u_f, \alpha=0)}$ and favored $e^{(f, \alpha=1)}$ Routhians as a function of the quadrupole pairing strength $G_{2\mu}$ relative to the value $G_{2\mu}^{sc}$ determined according to Ref. [26]. The calculations were performed for ^{120}Cs at fixed frequency and axial shape in order to address the effects of the QQ -pairing force alone. To find the origin of the signature inversion, we performed calculations with and without the mean-field contributions $\Gamma^{(2\mu)}$. The figure nicely demonstrates the role of the $\Gamma^{(22)}$ potential: It is the only component of $(\lambda\mu)$ that creates signature inversion of the order of a few tens of keV already at axial shape.

To gain a better understanding of the role played by the mean-field potential $\Gamma^{(2\mu)}$ as a function of neutron number, Fig. 2 shows the contribution to the signature splitting stemming from the Γ -potential $\Delta e_\Gamma = e_\Gamma^{(u_f, \alpha=0)} - e_\Gamma^{(f, \alpha=1)}$, where:

$$e_\Gamma^{(\alpha)} = \frac{1}{2} \text{Tr}(\Gamma^{(\alpha)} \rho^{(\alpha)}) \quad (4)$$

as a function of N in the $A \sim 130$ mass region (superscript (α) refers to the signature of the blocked $h_{11/2}$ quasi-particles). Neutron number $N=59$ corresponds to the occupation of the $\Omega = 1/2$ orbit, while at $N=75$ the $\Omega = 9/2$ orbit of the $h_{11/2}$ subshell becomes occupied. Note again, that axial, fixed deformation was chosen to address the role of the QQ -pairing force effects alone.

Obviously, the contribution Δe_Γ varies with the position of the Fermi energy. There is a clear tendency for all components of the pairing force to favor the unfavored signature. At the bottom of the $\nu h_{11/2}$ subshell (corresponding to $59 \leq N \leq 61$) the $\Gamma^{(20)}$, $\Gamma^{(21)}$ and even $\Gamma^{(00)}$ show trends (negative contributions) towards the anomalous signature splitting. In these cases, however, the signature splitting caused by the Coriolis force is considerably larger, implying that signature inversion cannot occur. Around the middle of the shell (corresponding to $63 \leq N \leq 69$) where the signature splitting induced by the Coriolis force is rather small or even absent at low rotational frequencies, the $\Gamma^{(22)}$ potential favors the inversion and may even compete with the Coriolis force. Note, that this corresponds to the neutron numbers where indeed the signature inversion has been observed experimentally, see e.g. Ref. [32] and references therein.

The signature splitting, $\Delta e'$, as a function of the neutron shell filling with and without QQ -pairing is shown in Fig. 3. The calculations were done at fixed *triaxial* shape of $\gamma = 15^\circ$ and at $\hbar\omega = 0.2$ MeV. Both sets of the calculations result in signature inversion for neutron numbers ≥ 63 . However, a clear increase in the anomalous splitting of the order ~ 40 keV is caused by the QQ -pairing force. The size of the signature inversion as a function of the triaxiality parameter γ for the case of ^{120}Cs can be studied in Fig. 4. Note, that the contribution due to the QQ -pairing is almost independent of γ due to double stretching [33]. In a previous work [10] on ^{120}Cs , the γ deformation obtained from the earlier TRS calculations (including only seniority pairing treated non-self-consistently and no number projection) could not account for the observed signature splitting. In the extended TRS calculations, the combined effects of triaxiality and QQ -pairing force reproduce the data in this nucleus very well [17].

For the $A \sim 130$ and $A \sim 160$ nuclei, the anomalous signature splitting happens at low rotational frequencies where the Coriolis mixing is weak. However, with increasing rotational frequency, the Coriolis force dominates always and restores signature splitting to normal order. The critical frequency, $\hbar\omega_c$, at which this takes place is another characteristic quantity of signature inversion. Fig. 5 shows a significant increase in $\hbar\omega_c$ due to the presence of QQ -pairing. Finally, Fig. 6 shows the effect of the QQ -pairing force on the total angular momentum I_x as a function of the shell filling. The calculations were performed at $\hbar\omega = 0.2$ MeV. In general, QQ -pairing slightly increases (decreases) I_x for the unfavored (favored) signature, respectively. Moreover, the effect is somewhat larger for the unfavored signature branch. Although globally the effect is rather modest, it clearly reduces the normal signature splitting or enhances anomalous signature splitting, depending on neutron number.

Let us make the following few remarks summarizing the discussion of this section. It seems rather well documented that signature inversion (in axially deformed nuclei) in our calculation is due to the $\Gamma^{(22)}$ potential. The effect is not

accidentally related to the particular choice of pairing strength parameters. Indeed, a change of G_{00} and(or) $G_{2\mu}$ (see Fig. 1) by $\pm 10\%$ only weakly affects the calculated value of $\Delta e'$. Our calculations also do not show that the effect is related to number-projection. Analogous calculations but performed within the BCS approximation led us to similar conclusions. However, it is of crucial importance to perform rigorous blocking for each signature separately. Indeed, approximating the odd-N system by a one quasiparticle state created on top of the odd-N vacuum does not result in any inversion. Blocking of signature partners at non-zero rotational frequency (where signature splitting due to time-reversal symmetry breaking sets in) leads to, in general small, differences in density matrices $\rho^{(\alpha_f)}$ and $\rho^{(\alpha_{uf})}$ which in turn result in differences between $\Gamma_{\alpha_f}^{(\lambda\mu)}$ and $\Gamma_{\alpha_{uf}}^{(\lambda\mu)}$ potentials for favored and unfavored signature bands, respectively. However, we were not able to recognize a simple mechanism causing the small differences in the density matrices to add up "coherently" and eventually form such a regular pattern as depicted in Figs. 1-6.

IV. THE TRS RESULTS: COMPARISON WITH EXPERIMENT FOR THE A~130 AND A~160 NUCLEI

In this section, we present the results from the pairing and deformation self-consistent TRS model described in Sec. II for the odd-odd $^{120-124}\text{Cs}$, $^{124-128}\text{La}$, $^{154-158}\text{Tb}$, $^{156-160}\text{Ho}$ and $^{158-162}\text{Tm}$ nuclei. In order to compare theory and experiment, the correct spin assignments of the bands are crucial. Indeed, by changing the spin values by one unit, the signature splitting becomes inverted and a totally different pattern emerges. Particularly in odd-odd nuclei, due to the complexity of the low-spin spectra, spins are not always directly determined in experiment. This is the case for many of the rotational bands associated with the $\pi h_{11/2} \otimes \nu h_{11/2}$ configuration in the $A \sim 130$ region and $\pi h_{11/2} \otimes \nu i_{13/2}$ configurations in the $A \sim 160$ region. Therefore, we start our discussion by revisiting current spin assignments in these bands.

As mentioned above, the spin assignments of many rotational bands associated with the $\pi h_{11/2} \otimes \nu h_{11/2}$ configuration in the $A \sim 130$ region and with the $\pi h_{11/2} \otimes \nu i_{13/2}$ in the $A \sim 160$ region are tentative and based mainly on systematics. However, if the underlying assumptions or "the first guesses" are false, incorrect assignment may spread over many nuclei. Indeed, the spin assignments in these nuclei are very controversial. In ^{128}La , for example, the recent experiment [34] firmly established the experimental spins via in-beam and β -decay measurements. The previous spin assignment of Ref. [35] was lower by $3\hbar$!

Our calculation is in good agreement with the experimental data in ^{128}La based on the recent spin assignment [34], see Fig. 8. Also for ^{120}Cs [10], very good agreement between calculations and experiment is achieved, see Fig. 8 and [17]. Therefore, we choose these two nuclei as the reference nuclei to verify spin assignments in the $\pi h_{11/2} \otimes \nu h_{11/2}$ bands in the Cs and La isotopes. We further assume in our analysis that nuclear moments of inertia $\mathcal{J}^{(1)} \equiv I_x/\omega(I)$ smoothly decrease with increasing neutron number. This assumption is supported by comparison with neighboring even-even nuclei and by deformation systematics [36], see also Fig. 10. Based on the systematic analysis and at the same time compared with our cranking calculations, new spin values are suggested as shown in Table I.

The experimental $\mathcal{J}^{(1)}$ moments of inertia for the Cs and La isotopes corresponding to our new assignments are shown in Fig. 7. They decrease smoothly with increasing Fermi energy. The sensitivity of the method is shown for the case of $^{130,132}\text{La}$. As is seen in Fig. 7, changing the spins by $\pm 1\hbar$ introduces rather sharp kinks in the sequence of the moments of inertia in these nuclei, imposing rather strong restrictions for the relative spin values between the different isotopes. This analysis can of course not replace any experimental verification, but at present corresponds to the most reliable way in the absence of accurate data.

We have also investigated the spin assignments for the $\pi h_{11/2} \otimes \nu i_{13/2}$ bands of $^{154,156}\text{Tb}$, $^{156-160}\text{Ho}$ and $^{158-162}\text{Tm}$. For this mass region, our calculations agree well with the bulk part of the data as well as the recent analysis [37]. Systematics of the empirical moments of inertia ($\mathcal{J}^{(1)}$ is expected to increase with neutron number in this mass region) and spins suggest that the experimental assignments of ^{158}Ho and ^{156}Tb are too low. Such assignments can in general not account for the initial alignment that one expects from low- Ω , high- j orbits. With the guidance of the available spin assignments and our cranking calculations, we suggest the spin values presented in Table I. The comparison between experimental (with our spin assignments) and theoretical values of I_x versus $\hbar\omega$ are shown in Figs. 8 and 9 for the A~130 and A~160 mass regions, respectively.

In Refs. [38,37], the spin assignments for the A~130 and A~160 nuclei were investigated by energy systematics. Our assignments are in general consistent with their results. However, Liu *et al.* give three different sets of assignments for the Cs isotopes depending on the choice of the reference nucleus [38]. One of the sets coincides with our result. Systematical changes in the assigned spin values (e.g. by $2\hbar$) do not change the (energy) systematics [38]. We have chosen ^{128}La [34] and the lighter isotope of ^{120}Cs [10] guided by theoretical results, see Fig. 8. This assignment is also consistent with the measurements for ^{130}Cs [39]. The nice agreement between the calculation and experiment (in particular for ^{128}La) gives some confidence for the present method, see Fig. 8. Especially the low spin-part agrees

rather well with the experimental data. The increase in angular momentum with frequency for the favored signature is in general too strong when compared to experiment.

Fig. 10 depicts the equilibrium deformation parameters β_2 and γ obtained from the TRS calculations. For the $A \sim 130$ nuclei, in general, the β_2 and γ deformations decrease with increasing neutron number. However, the nuclear shapes of some $A \sim 130$ nuclei are usually rather soft, which may lead to some inaccuracy in determining the equilibrium deformations as well as it may affect other observables, in particular I_x values. The calculated deformations of the two signatures are rather close, but one should be aware that this may not always be the case, see e.g. ^{122}Cs (Fig. 10).

For the $A \sim 160$ isotopes, the the β_2 (γ) deformation value is increasing (decreasing) with neutron number, N . This is consistent with the increase of the moments of inertia with N . The γ deformations of the $A \sim 160$ nuclei are rather small. With increasing N , the γ deformations are predicted to change from small positive to small negative values. For most cases, the calculations yield a decrease of the deformation with increasing rotational frequency.

The quality of the present calculations is nicely demonstrated in Fig. 11 and Fig. 12, where we compare experimental and calculated Routhians, e' . Especially for the Cs- and La-isotopes, the agreement is in general within 50 keV. For the case of the heavier Rare Earth nuclei, at relatively high frequency $\hbar\omega \geq 0.25$ MeV, the calculated Routhians do not agree well with the experimental data. The deviations between experiment and theory can be linked to the fact that the unblocked neutron $i_{13/2}$ crossings occur too early in the calculations for some cases.

We also compare the difference of the Routhians $\Delta e' = e'_f - e'_u$ obtained in the TRS-calculations and experiment, Fig. 13 and Fig. 14.¹ In order to calculate the experimental values of $\Delta e'(\hbar\omega)$ we performed a linear interpolation of the unfavoured Routhians e'_u at the frequency values of the favoured signature. Again, the agreement for the $A=120$ -130 region is quite good. On the other hand, for the Rare Earth nuclei, the inversion is calculated to continue to somewhat higher frequencies and also to be more pronounced than in experiment. However, given the rather modest values of the inversion, in general < 30 keV, one can be quite content with the results. Above the frequency of $\hbar\omega = 0.5$ MeV (not seen in Fig. 14), the inversion has disappeared for all cases considered here. The TRS-calculations clearly show that the mean-field model can account for the signature inversion phenomenon, once shape-polarization and pairing effects are treated self-consistently. The anomalous signature splitting is obtained already at almost axial shapes, due to the contribution of the $(\lambda\mu) = (22)$ QQ -pairing interaction to the single-particle potential. The overall agreement between theory and experiment appears satisfactory.

V. SUMMARY

We have demonstrated that shape and pairing self-consistent mean-field calculations can account for the rotational band structure of the unique parity high- j orbits in the odd-odd $A \sim 130$ and $A \sim 160$ nuclei. In particular, the signature inversion phenomenon is reproduced. The agreement between theory and the data is satisfactory provided that some of the empirical spin assignments are revised. New spins are suggested based on a systematic analysis of the $\mathcal{J}^{(1)}$ moments of inertia which rather firmly establishes relative spins along each isotopic chain considered here. The absolute spin values are finally determined partly guided (see Sec. IV) by theoretical values.

The experimental signature-splittings are quite well reproduced although the TRS calculations yield rather modest values of the triaxiality parameter γ ($\gamma < 5^\circ$) for most cases. This can be understood in terms of the additional enhancement of the anomalous signature splitting caused by the mean-field contribution of the $(\lambda\mu) = (22)$ component of the quadrupole pairing interaction, see Sec. III.

Some deficiencies of the model are clearly visible particularly at high rotational frequency and for γ -soft nuclei. Other effects, such as the coupling between rotation and γ -vibration, may need to be taken into account. Also more elaborate forces, in particular accounting for the valence neutron-proton interaction [11,13], might further improve the agreement to the data. For a full understanding of this intriguing phenomenon, the calculations of electromagnetic transitions rates are important. This, however, is beyond the scope of our work.

This work was supported by the Swedish Institute (SI), Swedish Natural Science Research Council (NFR), the Göran Gustafsson Foundation and the Polish Committee for Scientific Research (KBN) under Contract No. 2 P03B 040 14.

¹Note that here the sign of $\Delta e'$ is opposite to the one chosen in previous figures

- [1] A. Bohr and B.R. Mottelson, *Proc. Int. Conf. on nuclear structure*, Tokyo, Sep. 1977, J. Phys. Soc. Japan Suppl. **44** (1978) 157.
- [2] F.S. Stephens, *Rev. Mod. Phys.* **47** (1975) 43.
- [3] I. Hamamoto and B. Mottelson, *Phys. Lett.* **B167** (1986) 370.
- [4] R. Bengtsson, H. Frisk, F.R. May, and J.A. Pinston, *Nucl. Phys.* **A415** (1984) 189.
- [5] S. Frauendorf and F.R. May, *Phys. Lett.* **B125** (1983) 245.
- [6] I. Hamamoto and B. Mottelson, *Phys. Lett.* **B127** (1983) 281.
- [7] I. Hamamoto and B. Mottelson, *Phys. Lett.* **B132** (1983) 7.
- [8] A. Ikeda and S. Åberg, *Nucl. Phys* **A480** (1988) 85.
- [9] M. Matsuzaki, *Nucl. Phys.* **A504** (1989) 456.
- [10] B. Cederwall, F. Lidén, A. Johnson, L. Hildingsson, R. Wyss, B. Fant, S. Juutinen, P. Ahonen, S. Mitarai, J. Mukai, J. Nyberg, I. Ragnarsson, and P.B. Semmes, *Nucl. Phys.* **A542** (1992) 454.
- [11] I. Hamamoto, *Phys. Lett.* **B179** (1986) 327.
- [12] M. Matsuzaki, *Phys. Lett.* **B269** (1991) 23.
- [13] P.B. Semmes and I. Ragnarsson, *Proc. of Int. Conf. on High-Spin Phys. and Gamma-Soft Nuclei*, Pittsburgh, 1990 (World Scientific Pub., Singapore, 1991) pp. 500.
- [14] N. Tajima, *Nucl. Phys.* **A572** (1994) 365.
- [15] R.A. Bark, J.M. Espino, W. Reviol, P.B. Semmes, H. Carlsson, I.G. Bearden, G.B. Hagemann, H.J. Jensen, I. Ragnarsson, L.L. Riedinger, H. Ryde, and P.O. Tjøm, *Phys. Lett.* **B406** (1997) 193.
- [16] K. Hara and Y. Sun, *Nucl. Phys.* **A531** (1991) 221.
- [17] W. Satuła and R. Wyss, *Acta Phys. Polonica*, **B27** (1996) 121.
- [18] W. Nazarewicz, R. Wyss, and A. Johnson, *Nucl. Phys.* **A503** (1989) 285.
- [19] D.R. Inglis, *Phys. Rev.* **96** (1954) 1059; *Phys. Rev.* **97** (1955) 701.
- [20] V.M. Strutinsky, *Yad. Fiz.* **3** (1966) 614; *Nucl. Phys.* **A95** (1967) 420.
- [21] S. Ćwiok, J. Dudek, W. Nazarewicz, J. Skalski, and T.R. Werner, *Comp. Phys. Comm.* **46** (1987) 379.
- [22] S. Cohen, F. Plasil, and W.J. Swiatecki, *Ann. Phys. (NY)* **82** (1974) 557.
- [23] A.L. Goodman, *Nucl. Phys.* **A230** (1974) 466.
- [24] H.C. Pradhan, Y. Nogami, and J. Law, *Nucl. Phys.* **A201** (1973) 357.
- [25] P. Möller and R. Nix, *Nucl. Phys.* **A536** (1992) 20.
- [26] H. Sakamoto and T. Kishimoto, *Phys. Lett.* **B245** (1990) 321.
- [27] W. Satuła and R. Wyss, *Proceedings of the Conference on Physics from Large Gamma-ray Detector Arrays*, August 1994, Berkeley, Ca., USA, p. 157.
- [28] W. Satuła, R. Wyss, and P. Magierski, *Nucl. Phys.* **A578** (1994) 45.
- [29] W. Satuła and R. Wyss, *Phys. Rev.* **C50** (1994) 2888.
- [30] W. Satuła and R. Wyss, *Phys. Scripta* **T56** (1995) 159.
- [31] R. Wyss and W. Satuła, *Phys. Lett.* **B351** (1995) 393.
- [32] T. Komatsubara, K. Furuno, T. Hosoda, J. Mukai, T. Hayakawa, T. Morikawa, Y. Iwata, N. Kato, J. Espino, J. Gascon, N. Gjørup, G.B. Hagemann, H.J. Jensen, D. Jerrestam, J. Nyberg, G. Slettern, B. Cederwall, and P.O. Tjøm, *Nucl. Phys.* **A557** (1993) 419c.
- [33] W. Satuła, R. Wyss, and F. Döna, *Nucl. Phys.* **A565** (1993) 573.
- [34] T. Hayakawa, J. Lu, J. Mukai, T. Saitoh, N. Hasimoto, T. Komatsubara, and K. Furuno, *Z. Phys.* **A352** (1995) 241.
- [35] M. J. Godfrey, Y. He, I. Jenkins, A. Kirwan, P.J. Nolan, D.J. Thornley, S.M. Mullins, and R. Wadsworth, *J. Phys.* **G15** (1989) 671.
- [36] R. Wyss, A. Granderath, W. Lieberz, R. Bengtsson, P. von Brentano, A. Dewald, A. Gelberg, A. Gizon, J. Gizon, S. Harrisopulos, A. Johnson, W. Nazarewicz, J. Nyberg, and K. Schiffer, *Nucl. Phys.* **A505** (1989) 337.
- [37] Yunzuo Liu, Yingjun Ma, Hongting Yang, and Shangui Zhou, *Phys. Rev.* **C52** (1995) 2514.
- [38] Yunzuo Liu, Jingbin Lu, Yingjun Ma, Shangui Zhou, and Hua Zheng, *Phys. Rev.* **C54** (1996) 719.
- [39] P.R. Sala, N. Blasi, G.Lo Bianco, A. Mazzoleni, R. Reinhardt, K. Schiffer, K.P. Schmittgen, G. Siems, and P.Von Brentano, *Nucl. Phys.* **A531** (1991) 383.
- [40] N. Xu, Y. Liang, R. Ma, E.S. Paul, and D.B. Fossan, *Phys. Rev.* **C41** (1990) 2681.
- [41] E.S. Paul, D.B. Fossan, Y. Lian, R. Ma, and N. Xu, *Phys. Rev.* **C40** (1989) 619.
- [42] B.M. Nyako, J. Gizon, D. Barneoud, A. Gizon, M. Jozsa, W. Klamra, F.A. Beck, and J.C. Merdinger, *Z. Phys.* **A332** (1989) 235.
- [43] E.S. Paul, C.W. Beausang, D.B. Fossan, R. Ma, W.F. Piel Jr., and N. Xu, *Phys. Rev.* **C36** (1987) 1853.
- [44] J.R.B. Oliveria, L.G.R. Emediato, M.A. Rizzutto, R.V. Ribas, W.A. Seale, M.N. Rao, N.H. Medina, S. Botelho, and E.W. Cybulska, *Phys. Rev.* **C39** (1989) 2250.
- [45] J.R.B. Oliveira, L.G.R. Emediato, E.W. Cybulska, R.V. Ribas, W.A. Seale, M.N. Rao, N.H. Medina, M.A. Rizzutto, S. Botelho, and C.L. Lima, *Phys. Rev.* **C45** (1992) 2740.
- [46] R. Bengtsson, J.A. Pinston, D. Barneoud, E. Monnard, and F. Schussler, *Nucl. Phys.* **A389** (1982) 158.
- [47] R.G. Helmer, *Nucl. Data Sheets* **65** (1992) 94.

- [48] R.G. Helmer, Nucl. Data Sheets **77** (1996) 574.
- [49] J.L. Salicio, M. Déléze, S. Drissi, J. Kern, S.J. Mannanal, J.P. Vorlet, and I. Hamamoto, Nucl. Phys. **A512** (1990) 109.
- [50] S. Drissi, A. Bruder, J.Ci. Dousse, V. Ionescu, J. Kern, J.A. Pinston, S. Andre, D. Barneoud, J. Genevey, and H. Frisk, Nucl. Phys. **A451** (1986) 313.

TABLE I. Assigned spins and parities for the lowest observed levels of the $\pi h_{11/2} \otimes \nu h_{11/2}$ bands in the Cs and La isotopes and the $\pi h_{11/2} \otimes \nu i_{13/2}$ bands in the A~160 nuclei. The references for the previous assignments are shown in brackets.

Nuclei	¹²⁰ Cs	¹²² Cs	¹²⁴ Cs	¹²⁶ Cs	¹²⁸ Cs	¹³⁰ Cs		
Previous	8 ⁺ [10]	6 ⁻ [40] ^a	7 ⁺ [32]	5 ⁺ [32]	9 ⁺ [41]	9 ⁺ [39]		
Present	8 ⁺	9 ⁺	9 ⁺	9 ⁺	10 ⁺	9 ⁺		
Nuclei	¹²⁴ La	¹²⁶ La	¹²⁸ La	¹³⁰ La	¹³² La	¹³⁴ La		
Previous	7 ⁺ [38]	4 ⁺ [42]	5 ⁺ [34]	8 ⁺ [43]	8 ⁺ [44]	8 ⁺ [45]		
Present	7 ⁺	7 ⁺	5 ⁺	9 ⁺	9 ⁺	9 ⁺		
Nuclei	¹⁵⁴ Tb	¹⁵⁶ Tb	¹⁵⁶ Ho	¹⁵⁸ Ho	¹⁶⁰ Ho	¹⁵⁸ Tm	¹⁶⁰ Tm	¹⁶² Tm
Previous	9 ⁻ [46]	6 ⁻ [46]	9 [47]	6 ⁻ [48]	6 ⁻ [49]	9 ⁻ [50]	9 ⁻ [50]	7 ⁻ [50]
Present	9 ⁻	8 ⁻	9 ⁻	9 ⁻	6 ⁻	9 ⁻	9 ⁻	7 ⁻

^aThis band was assigned in Ref. [40] as $\pi h_{11/2} \otimes \nu g_{7/2}$ and later reassigned as the $\pi h_{11/2} \otimes \nu h_{11/2}$ configuration in Refs. [32,38]. The present calculation supports the $\pi h_{11/2} \otimes \nu h_{11/2}$ configuration assignment.

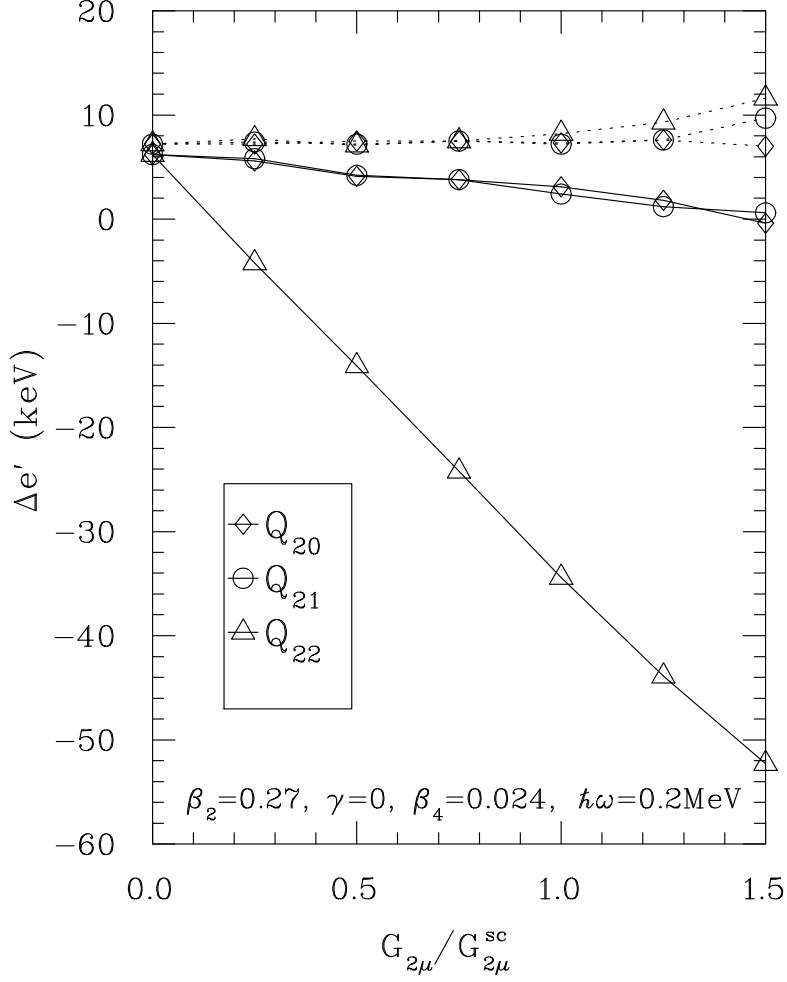


Fig.1, Xu

FIG. 1. The contribution of each $Q_{2\mu}$ component to the signature splitting in ^{120}Cs as a function of the QQ -pairing force strength $G_{2\mu}/G_{2\mu}^{\text{sc}}$, ($\mu = 0, 1, 2$). The $G_{2\mu}^{\text{sc}}$ is the strength of QQ -pairing determined according to the prescription of Ref. [26]. Calculations have been performed at $\hbar\omega=0.20$ MeV. The β_2 and β_4 parameters correspond to the equilibrium deformation obtained in the TRS calculations but the γ deformation was set to zero in order to address the effects of the QQ -pairing force alone. The solid/dotted lines mark calculations with/without the $\Gamma^{(2\mu)}$ potential. The negative value of $\Delta e'$ implies the occurrence of signature inversion.

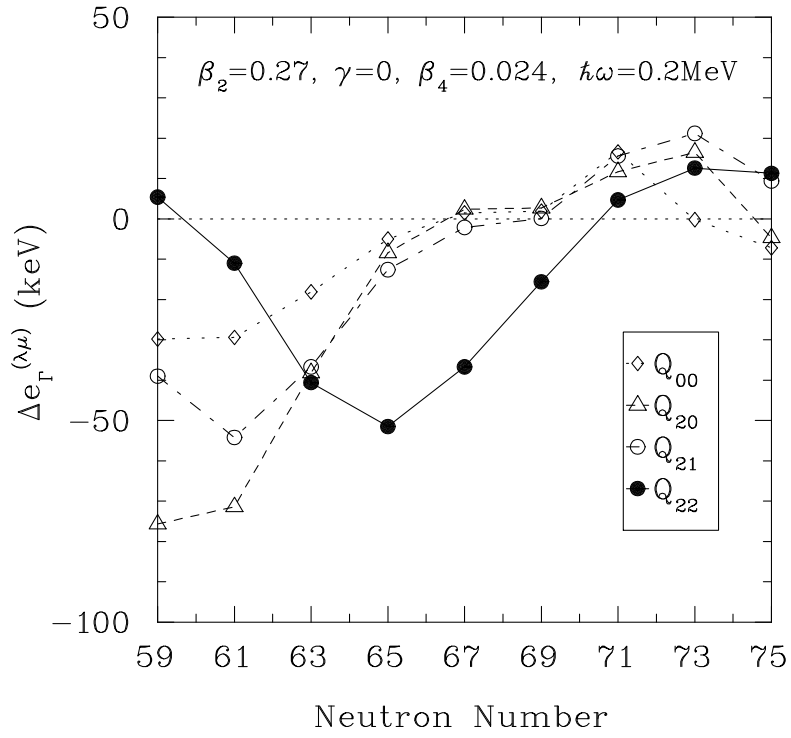


Fig.2, Xu

FIG. 2. The contribution of each component of the $\Gamma^{(\lambda\mu)}$ potential (see text for details) to the signature splitting in $A\sim 130$ nuclei as a function of neutron number.

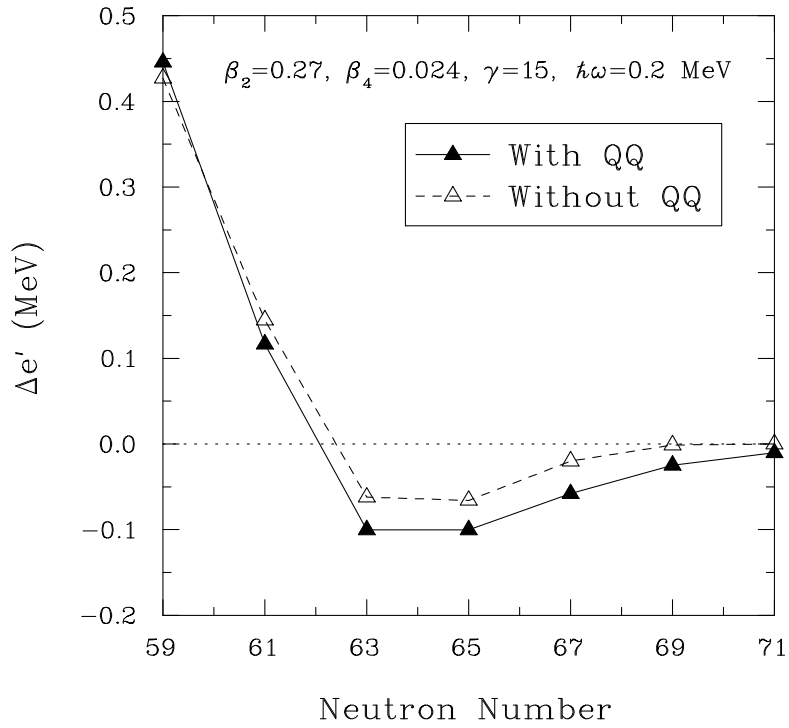


Fig.3, Xu

FIG. 3. Signature splitting between the unfavored and favored levels of the $h_{11/2}$ quasi-neutron as a function of neutron shell filling. Rotational frequency and deformation (triaxial) were kept constant. Calculations with (without) the QQ -pairing interaction are marked by solid (dashed) line and filled (open) triangles, respectively.

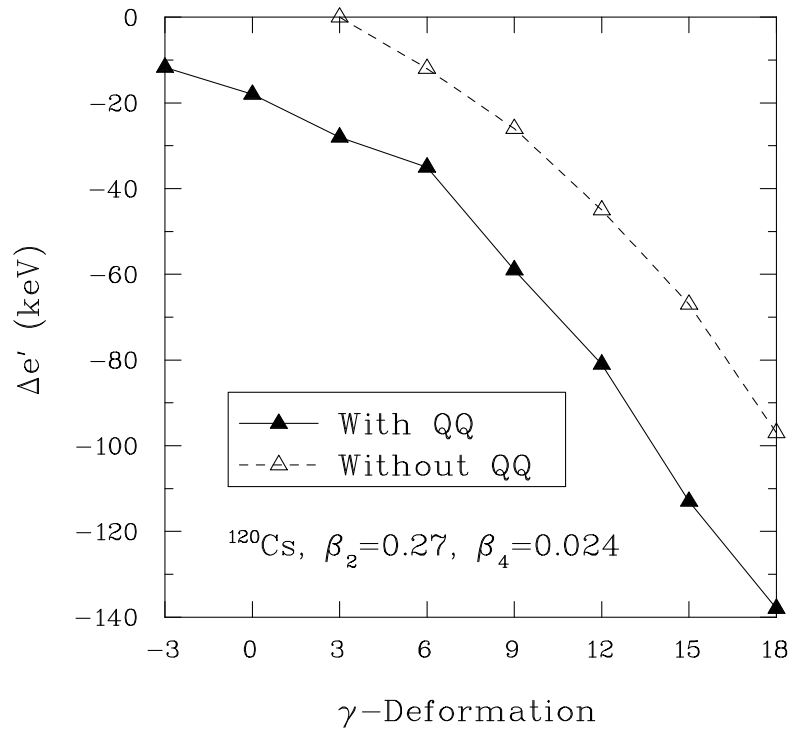


Fig.4, Xu

FIG. 4. The variation of the signature splitting versus γ deformation for ^{120}Cs .

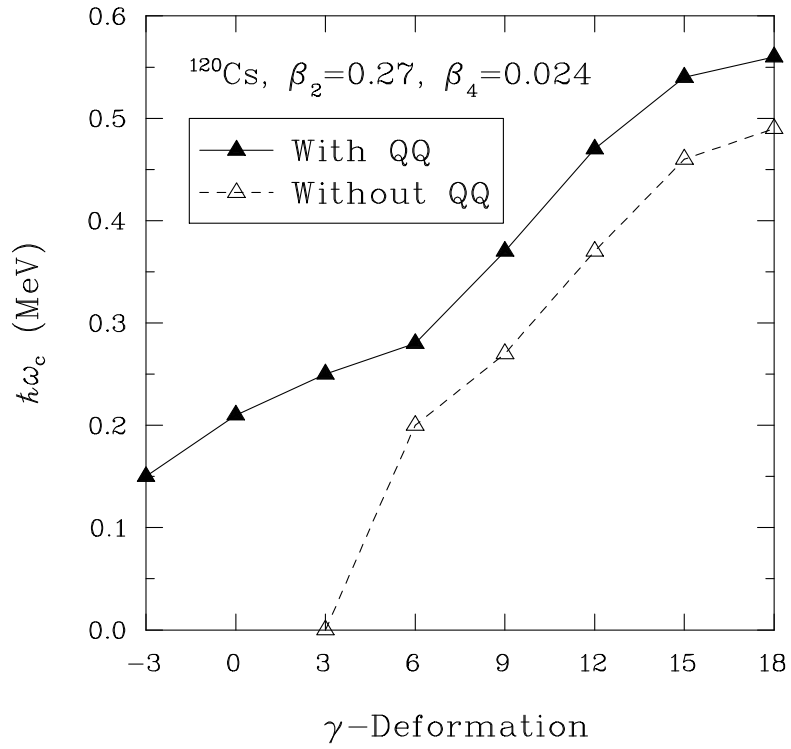


Fig.5, Xu

FIG. 5. The critical frequency, $\hbar\omega_c$, at which the normal signature splitting is restored as a function of triaxiality γ .

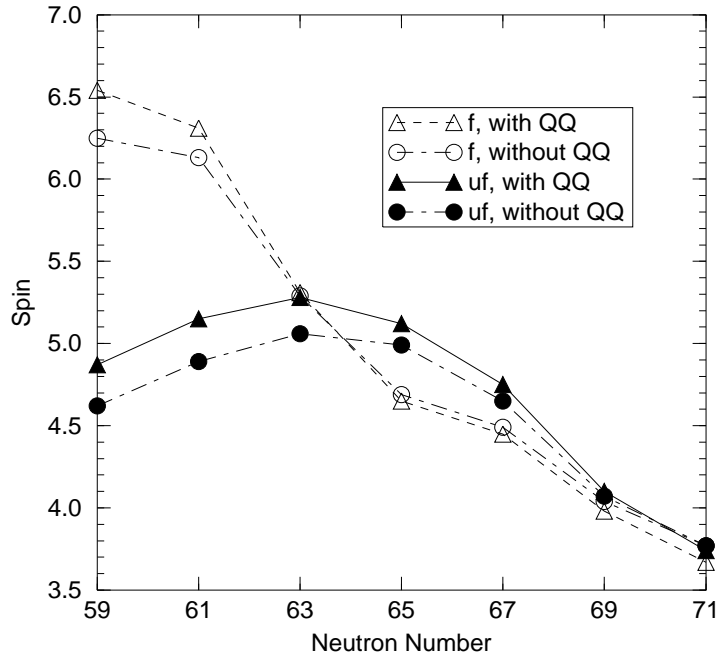


Fig.6, Xu

FIG. 6. The neutron contribution to the total angular momentum of the favored (f) and unfavored (uf) signature bands as a function of neutron number at $\hbar\omega = 0.2$ MeV. The deformation is set to the same values as in Fig. 3.

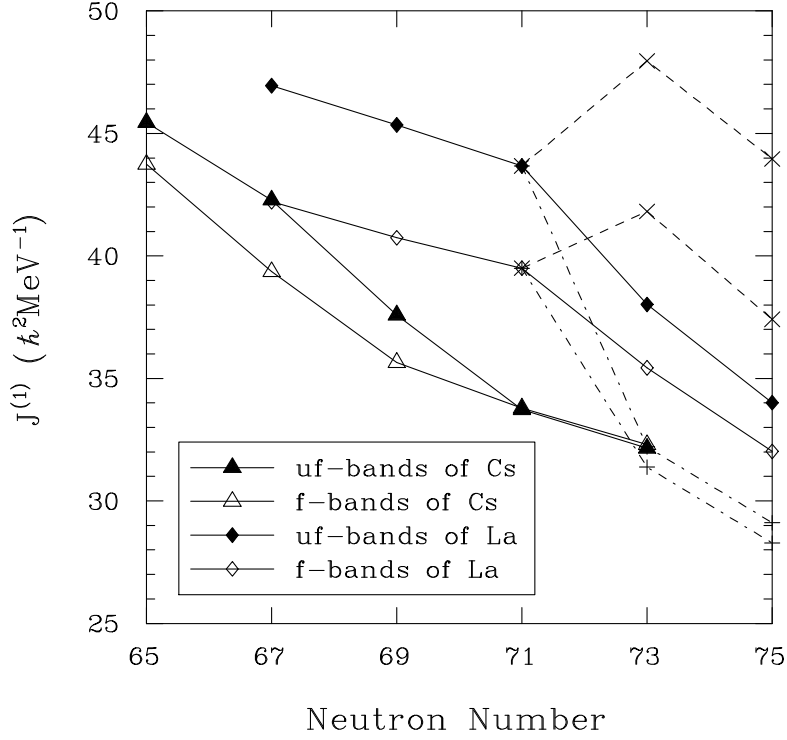


Fig.7, Xu

FIG. 7. The experimental moments of inertia for the Cs (filled symbols) and La (open symbols) isotopes corresponding to our spin assignments following the discussion in Sec. IV. For the favored (unfavored) bands, the $\mathcal{J}^{(1)}$ values at $I = 11(10)\hbar$ are plotted, respectively. The dashed (dot-dashed) curves indicate variations in $\mathcal{J}^{(1)}$ of $^{130,132}\text{La}$ caused by changes in the spin values by $+1(-1)\hbar$, respectively.

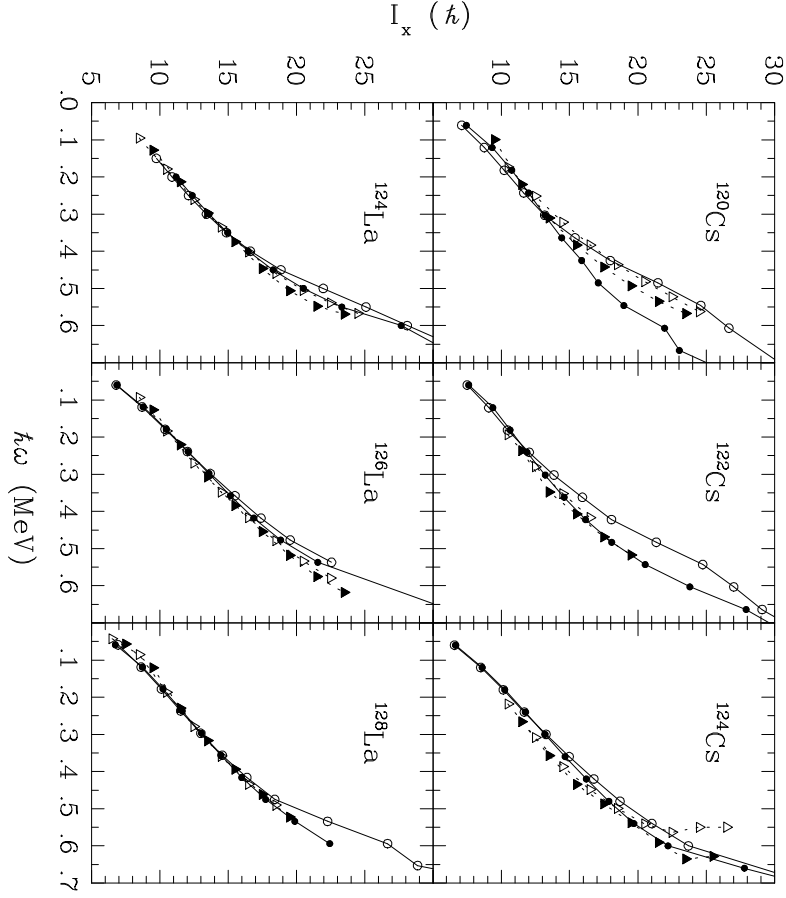


Fig.8, Xu

FIG. 8. Experimental and calculated total angular momenta (I_x) for the $\pi h_{11/2} \otimes \nu h_{11/2}$ bands in odd-odd $^{120-124}\text{Cs}$ and $^{124-128}\text{La}$ nuclei. The triangles (empty and filled) correspond to the experimental data (favored and unfavored signatures, respectively). The circles (empty and filled) mark the TRS results (favored and unfavored signatures, respectively). Our new spin assignments (Sec. IV) are used. The references to the original data are found in Table I.

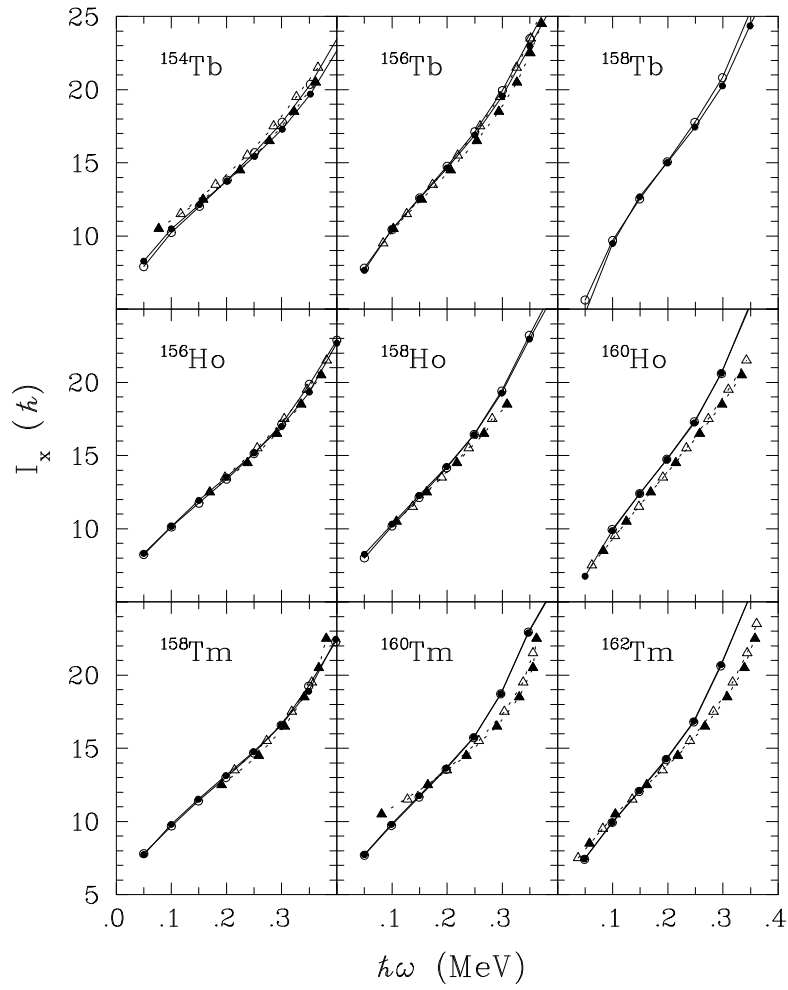


Fig.9, Xu

FIG. 9. Similar to Fig. 8, but for the $\pi h_{11/2} \otimes \nu i_{13/2}$ bands in the $A \sim 160$ nuclei.

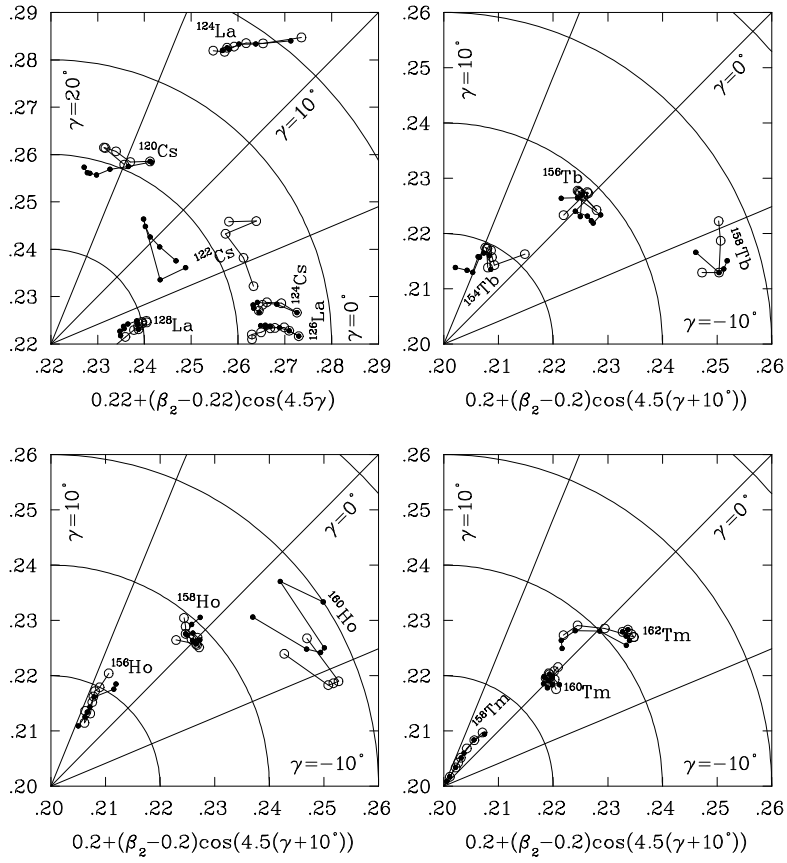


Fig.10, Xu

FIG. 10. The calculated quadrupole equilibrium deformations β_2 and γ for the $\pi h_{11/2} \otimes \nu h_{11/2}$ and $\pi h_{11/2} \otimes \nu i_{13/2}$ rotational bands. The empty (filled) circles are for favored (unfavored) bands, respectively.

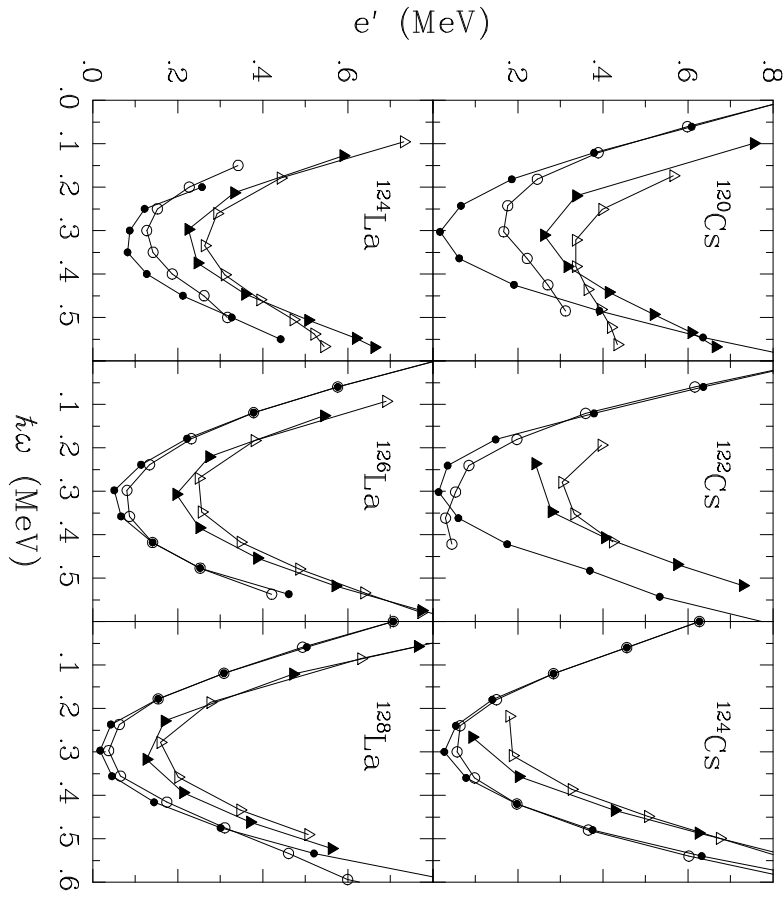


Fig.11, Xu

FIG. 11. Experimental and calculated Routhians for the $\pi h_{11/2} \otimes \nu h_{11/2}$ bands in Cs and La isotopes as a function of rotational frequency. A common reference Routhian of $J_0 = 44 \hbar^2 \text{MeV}^{-1}$ has been subtracted. The triangles (empty and filled) mark the experimental data (favored and unfavored signatures, respectively), while (empty and filled) circles denote the TRS results (favored and unfavored signatures, respectively). The assignments of Sec. IV have been used. Note, that the normalization of the Routhians is arbitrary.

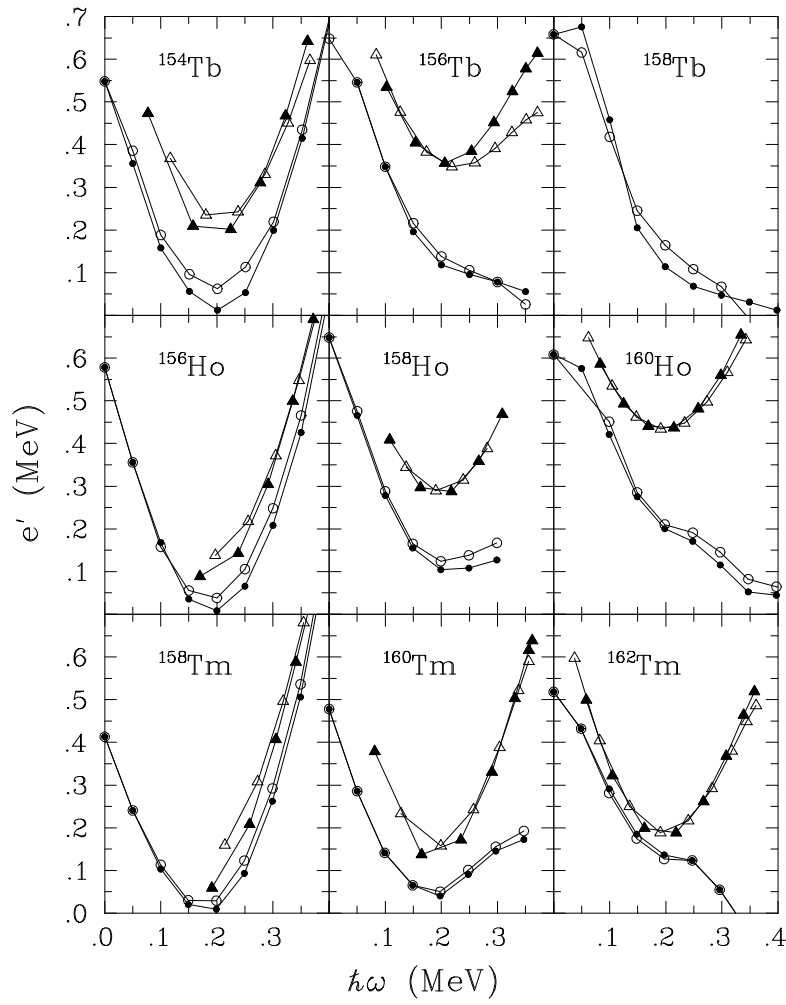


Fig.12, Xu

FIG. 12. Similar to Fig. 11, but for the $\pi h_{11/2} \otimes \nu i_{13/2}$ bands in $A \sim 160$ nuclei. The inertia parameter of the subtracted reference Routhian is $J_0 = 70 \hbar^2 \text{MeV}^{-1}$.

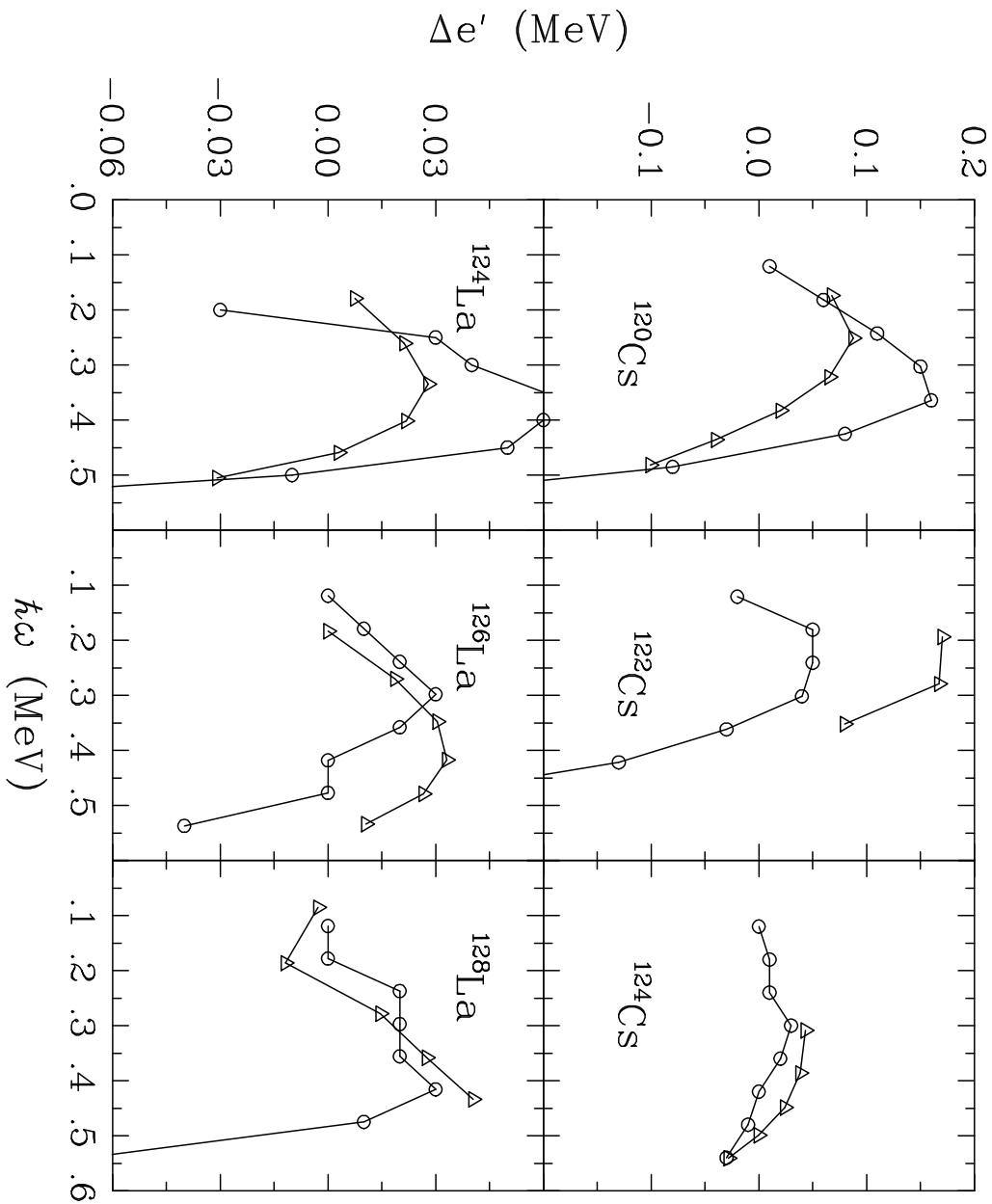


FIG. 13. The difference of calculated and experimentally deduced Routhians from Fig. 11, $\Delta e' = e'_f - e'_u$, where f (u) stands for (un-)favoured signature. Positive values of $\Delta e'$ correspond to signature inversion. The triangles (circles) characterize experimental (calculated) values. Note that the scales for the Cs- and La-isotopes are different.

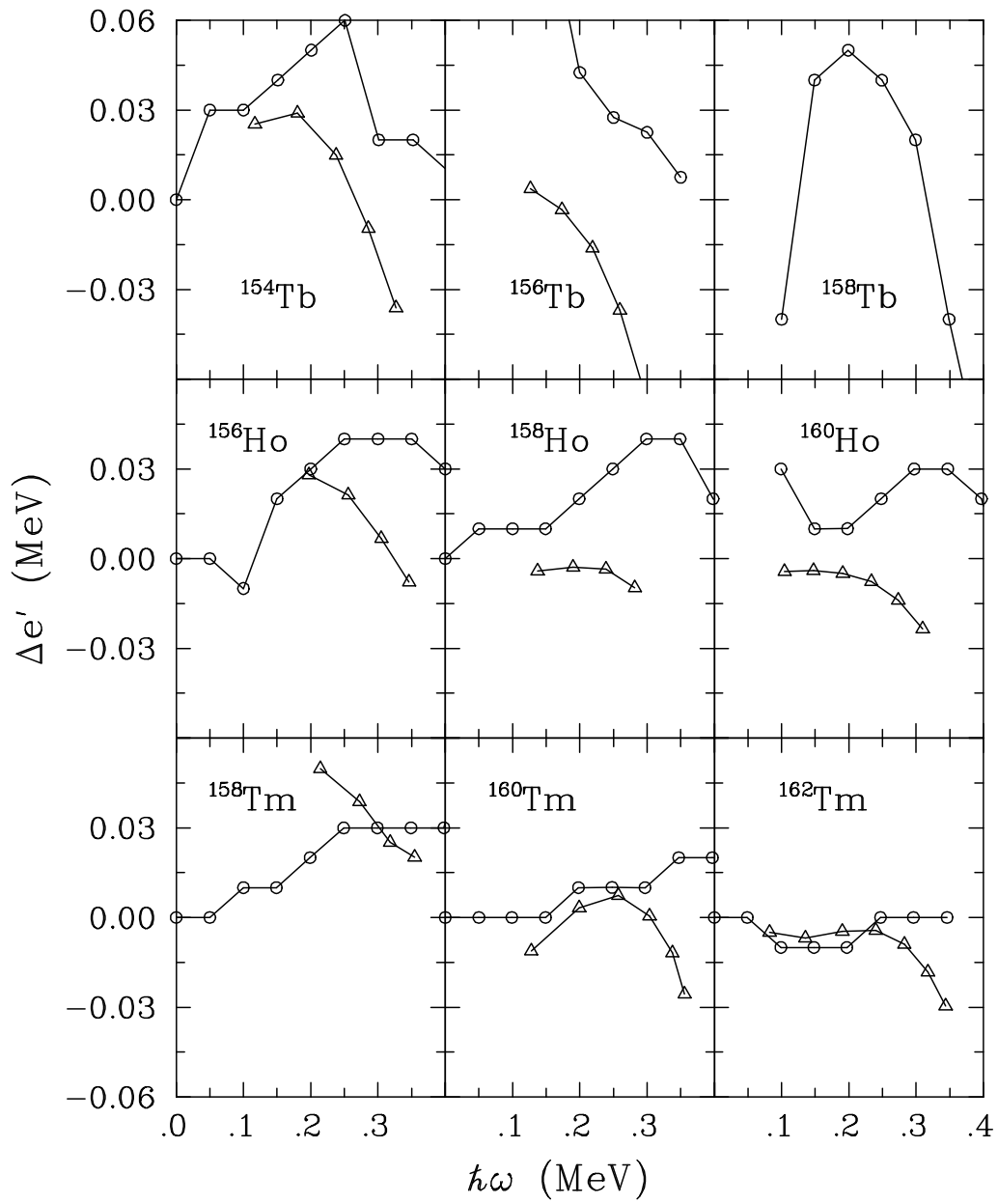


FIG. 14. Similar to Fig. 13, but for the $\pi h_{11/2} \otimes \nu i_{13/2}$ bands in $A \sim 160$ nuclei.